Cement & Concrete Composites 34 (2012) 121–130

Contents lists available at SciVerse ScienceDirect

Cement & Concrete Composites

journal homepage: www.elsevier.com/locate/cemconcomp

# Roles of water film thickness and SP dosage in rheology and cohesiveness of mortar

A.K.H. Kwan *, W.W.S. Fung

*Department of Civil Engineering, The University of Hong Kong, Hong Kong, China*

ARTICLE INFO

*Article history:*
Received 11 April 2010
Received in revised form 17 September 2011
Accepted 21 September 2011
Available online 29 September 2011

*Keywords:*
Cohesiveness
Mortar
Rheology
Superplasticizer

ABSTRACT

In recent studies, the authors have demonstrated that the combined effects of water content, packing density and solid surface area on the rheology of mortar may be evaluated in terms of the water film thickness (WFT). However, in addition to these factors, the superplasticizer (SP) dosage also has some effects. In order to study the roles of the WFT and SP dosage in the rheology and cohesiveness of mortar, a number of cement–sand mortar samples with different SP dosages and water contents were made for packing density, rheology and cohesiveness measurements. The results showed that the packing density and WFT would increase significantly with the SP dosage. At low SP dosage, the rheology of mortar is dependent on both the WFT and SP dosage while at high SP dosage, the rheology of mortar is dependent solely on the WFT. On the contrary, the cohesiveness of mortar is always dependent on both the WFT and SP dosage. Lastly, regression analysis of the test results was carried out and very good correlations of the measured rheological parameters to the WFT and SP dosage have been achieved.



## 1. Introduction

Since its advent in the 1960s, superplasticizer (SP) has played a pivotal role in the development of concrete technology [1,2]. After decades, it has evolved from the first generation known as plasticizer to the more effective second generation called SP [3]. Recently, polycarboxylate-based SP (PC-based SP) has also been developed as the third generation SP. With a SP added, the flowability of concrete can be improved. Alternatively, at the same flowability requirement, the water/cement (W/C) ratio can be reduced to improve the strength and durability of concrete. In this regard, Neville [4] remarked that it is the lower W/C ratio that makes a concrete a higher performance one. In such case, an effective SP has to be added to compensate for the reduced flowability. Because of these benefits, SP has become an indispensable ingredient for the production of modern concrete, especially high-performance concrete.

In simple terms, a SP works by dispersing the solid particles in the concrete. When no SP is added, the solid particles would tend to form agglomerates, thereby causing the solid particles to be loosely packed. When a SP is added to disperse the solid particles, agglomeration would be reduced, thus allowing the solid particles to be more closely packed. Therefore, the dispersion effect of the SP should improve the packing density of the solid particles. However, such potential improvement in the packing density of the solid particles, or more specifically, the cementitious materials plus aggregate particles, has never been studied so far. This is probably due to the lack of an appropriate test method for packing density measurement that is capable of incorporating the effect of SP.

The conventional methods of packing density measurement, as stipulated in the British Standard BS 812: Part 2: 1995 and Eurocode EN 1097-4: 1999, measure the packing density of the solid particles under dry condition. These methods, which may be classified as dry packing methods, are not applicable to materials containing fine particles, such as cementitious materials and fine aggregate. This is because under dry condition, the fine particles tend to form agglomerates and the packing density so measured is very sensitive to the compaction applied [5]. More importantly, the effects of water and SP in the concrete mix cannot be included. To resolve these problems, the author's research group has recently developed a new method, called the wet packing method, for measuring the packing densities of cementitious materials [6], fine aggregate [7] and cementitious materials plus fine aggregate [8] with the effects of water and SP included.

As mentioned before, the SP is to disperse the solid particles. This is effected through electrostatic repulsion produced by imparting similar electrostatic charges to the particles and, for a PC-based SP, also steric repulsion produced by wrapping the particles with co-polymer side chains [9]. Such dispersion of the solid particles would directly increase the flowability of the concrete. At the same time, the reduced agglomeration due to such dispersion would increase the packing density and thus the amount of excess water (water in excess of that needed to fill up the voids between the solid particles) in the concrete. Since it is the excess water that would provide a thin film of water coating each solid particle to lubricate the concrete, the increase in the amount of

* Corresponding author. Tel.: +852 2859 2647; fax: +852 2559 5337.
*E-mail addresses:* khkwan@hku.hk (A.K.H. Kwan), wilsonfl@graduate.hku.hk (W.W.S. Fung).

0958-9465/$ - see front matter © 2011 Elsevier Ltd. All rights reserved.
doi:10.1016/j.cemconcomp.2011.09.016

excess water would increase the water film thickness (WFT) and eventually further increase the flowability of the concrete.

The concepts of packing density and WFT are not new. Thirty years ago, Helmuth [10] suggested that it should be the thickness of water films coating the cement grains that governs the consistence of cement paste. Later in 1996, Zhang et al. [11] pointed out that the mixing water may be divided into two portions: one portion is the filling water, which fills into the voids between particles and does not contribute to fluidity, while the other portion is the excess water, which forms a water film on the surface of each particle and contributes to fluidity. Recently, there appears to be a revived interest in these concepts. For instance, Nanthagopalan et al. [12] in 2008 studied the effects of packing density on the flowability of cement paste and Peng et al. [13] in 2009 studied the effects of supplementary cementitious materials on the packing density of cementitious materials. However, there has been no research on how the SP dosage would affect the packing density and WFT, and how the SP dosage and WFT would affect the rheology of cement paste, mortar and concrete.

In recent studies, with the packing density measured using the wet packing method and the WFT determined as the excess water to solid surface area ratio, the author's research group has demonstrated that the WFT is the single most important factor governing the rheology of cement paste [14,15], cement–sand mortar [16] and condensed silica fume mortar [17]. As any SP added would disperse the solid particles, the SP dosage should also be a major factor. In other words, both the WFT and SP dosage should be playing certain roles in the rheology of superplasticized cement paste, mortar and concrete. On the other hand, whilst the dispersion effect of SP would improve the flowability, it would also impair the cohesiveness [18]. Hence, it may be expected that as the SP dosage increases, the cohesiveness would decrease, and sooner or later, segregation would occur. To avoid segregation, Aïtcin [19] recommended that the usage of any SP should be limited to its saturation dosage. However, the authors believe that the WFT should be limited too because it also has some effects on the cohesiveness.

In order to address the above issues, the present study was launched to investigate the effects of a PC-based SP on the rheology, cohesiveness and packing density of cement–sand mortar. A series of mortar samples, each representing the mortar portion of a concrete, were made for flowability, rheological properties, cohesiveness and packing density measurements. Based on the test results, the WFT of each mortar sample was evaluated as the excess water to solid surface area ratio and then the flowability, rheological properties and cohesiveness of the mortar samples were correlated to the WFT and SP dosage for regression analysis. The correlation revealed that the SP dosage has significant effects on the packing density and WFT while the WFT and SP dosage have inter-dependent and governing effects on the flowability, rheological properties and cohesiveness.

## 2. Testing programme

In the testing programme, 6 different SP dosages of 0%, 0.5%, 1.0%, 1.5%, 2.0% and 3.0% in terms of liquid mass of SP by mass of the cementitious materials were adopted for the design of the mortar samples (the recommended normal dosage by the supplier is 0.5–3.0%). An ordinary portland cement (OPC) was used as the only cementitious material and the cement to fine aggregate ratio was fixed at 0.75 by volume in order to exclude the effect of variation in fine aggregate content. The water content in terms of water/solid (W/S) ratio by volume was varied within the range of 0.35–0.85 (W/S ratio by weight within the range of 0.126–0.307) depending on the SP dosage. Altogether, 35 cement–sand mortar samples were produced for testing, as listed in Table 1. For easy identification, each mortar sample is assigned a designation of X–Y, in which X denotes the SP dosage as a percentage by mass of the cementitious materials and Y denotes the W/S ratio by volume. For example, 1.5–0.50 designates the mortar sample with a SP dosage of 1.5% and a W/S ratio of 0.50.

Each mortar sample was produced by mixing the ingredients in a standard mixer complying with BSEN 196: Parts 1–3. To ensure thorough mixing, a special mixing procedure of adding the solid materials in several small increments to the water was adopted. The author's research group has been using this method of mixing in previous studies [7,8,20] because the conventional method of mixing all the solid materials with water in a single batch would encounter difficulties when the water content is low and/or the SP dosage is low due to the apparent dryness of the mixture formed. The whole sample preparation and testing procedures were carried out in a laboratory maintained at a temperature of 24 ± 2 °C.

## 3. Materials

The OPC used was of strength class 52.5 N and had been tested to comply with BS 812: 1996. As for the fine aggregate, crushed granite rock fine with a maximum size of 1.18 mm and a water absorption of 1.6% by mass was used. The relative densities of the OPC and fine aggregate had been measured in accordance with BS 812: Part 2: 1995 as 3.11 and 2.66, respectively, whereas the Blaine fineness of the OPC had been measured in accordance with BSEN 196-6: 1992 as 345 $m^2$/kg. A laser diffraction particle size analyzer was used to measure the particle size distributions of the materials and the results are plotted in Fig. 1. Based on these particle size distributions, the specific surface areas of the OPC and fine aggregate were calculated to be $1.5415 \times 10^6$ and $0.2092 \times 10^6$ $m^2/m^3$, respectively. The SP employed was a PC-based SP with a solid mass content of 20% and a relative density of 1.03.

## 4. Test methods

### *4.1. Measuring flow spread and flow rate*

The mini slump cone and mini V-funnel tests were used to measure the flow spread and flow rate, respectively, of the mortar samples. There are several versions of mini slump cone and mini V-funnel. The versions adopted herein are the same as those used by Okamura and Ouchi [21], whose details are shown in Fig. 2.

For performing the mini slump cone test, the mortar was first poured into the slump cone until the slump cone was completely filled. Then, the slump cone was gently lifted to allow the mortar to flow and spread. After at least 3 min, the average diameter of the mortar patty formed was measured as the average of two perpendicular diameters. Finally, the flow spread was calculated as the average diameter of the mortar patty minus the base diameter of the slump cone.

For performing the mini V-funnel test, the mortar was first poured into the V-funnel with its bottom opening closed until the V-funnel was completely filled. Then, the bottom opening of the V-funnel was opened to allow the mortar to flow out. The time from the start of flow to the first sight of light through the bottom opening was recorded as the flow time. Finally, the flow rate was calculated as the volume of mortar sample (equal to 1134 ml) divided by the flow time.

### *4.2. Measuring rheological properties*

The vane test was used to evaluate the rheological properties of the mortar samples. It was carried out using a speed-controlled

**Table 1**
Flowability, rheological properties and cohesiveness results.

| Sample number | Flow spread (mm) | Flow rate (ml/s) | Yield stress (Pa) | Apparent viscosity (Pas) | SSI (%) |
|---|---|---|---|---|---|
| 0–0.65 | 0 | 0 | 51.59 | 6.41 | 0.0 |
| 0–0.70 | 14 | 263 | 41.81 | 4.85 | 0.0 |
| 0–0.75 | 62 | 532 | 20.73 | 3.32 | 3.1 |
| 0–0.80 | 94 | 741 | 21.92 | 2.31 | 5.0 |
| 0–0.85 | 128 | 886 | 15.15 | 1.78 | 16.6 |
| 0.5–0.45 | 0 | 0 | >100 | >50 | 0.0 |
| 0.5–0.50 | 0 | 42 | 70.65 | 14.59 | 0.0 |
| 0.5–0.55 | 83 | 161 | 27.78 | 7.98 | 0.0 |
| 0.5–0.60 | 147 | 337 | 13.54 | 4.28 | 0.0 |
| 0.5–0.65 | 178 | 497 | 8.21 | 2.97 | 0.5 |
| 0.5–0.70 | 211 | 648 | 3.50 | 1.53 | 5.6 |
| 0.5–0.75 | 234 | 886 | 2.61 | 0.84 | 16.0 |
| 1.0–0.40 | 0 | 0 | >100 | >50 | 0.0 |
| 1.0–0.45 | 141 | 152 | 13.45 | 9.02 | 0.0 |
| 1.0–0.50 | 193 | 231 | 4.37 | 4.31 | 0.0 |
| 1.0–0.55 | 224 | 312 | 2.41 | 2.74 | 0.2 |
| 1.0–0.60 | 242 | 408 | 1.53 | 1.79 | 4.1 |
| 1.0–0.65 | 255 | 603 | 1.67 | 1.48 | 14.9 |
| 1.5–0.40 | 84 | 68 | 30.39 | 19.76 | 0.0 |
| 1.5–0.45 | 215 | 161 | 4.10 | 5.53 | 0.0 |
| 1.5–0.50 | 247 | 237 | 2.44 | 3.60 | 0.1 |
| 1.5–0.55 | 264 | 320 | 1.00 | 2.64 | 4.2 |
| 1.5–0.60 | 275 | 426 | 0.07 | 1.95 | 11.8 |
| 2.0–0.35 | 63 | 27 | 30.08 | 32.20 | 0.0 |
| 2.0–0.40 | 259 | 88 | 10.24 | 11.82 | 0.0 |
| 2.0–0.45 | 263 | 169 | 2.16 | 4.86 | 0.2 |
| 2.0–0.50 | 286 | 230 | 1.84 | 3.76 | 5.4 |
| 2.0–0.55 | 280 | 336 | 0.79 | 1.80 | 9.2 |
| 2.0–0.60 | 284 | 443 | 0.79 | 1.59 | 14.4 |
| 3.0–0.35 | 204 | 48 | 14.12 | 22.52 | 0.0 |
| 3.0–0.40 | 272 | 127 | 4.24 | 7.08 | 1.4 |
| 3.0–0.45 | 286 | 188 | 2.86 | 4.85 | 11.2 |
| 3.0–0.50 | 288 | 275 | 2.09 | 2.52 | 14.9 |
| 3.0–0.55 | 294 | 350 | 1.00 | 2.02 | 24.0 |
| 3.0–0.60 | 295 | 450 | 0.95 | 1.15 | 34.0 |

*Note*: In the sample number X–Y, X denotes the SP dosage as a percentage by mass of the cementitious materials and Y denotes the W/S ratio by volume.

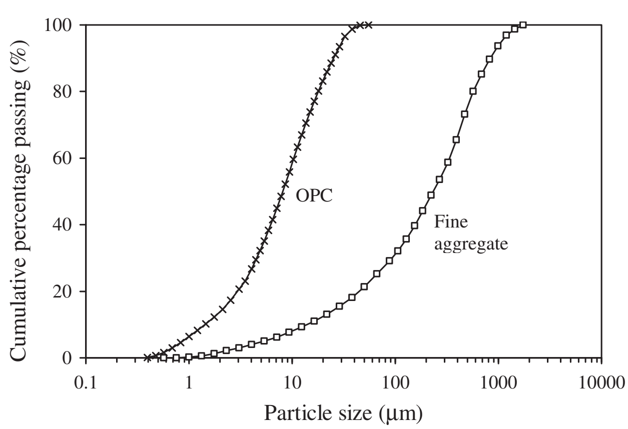


**Fig. 1.** Particle size distributions of OPC and fine aggregate.

rheometer equipped with a shear vane, measuring 20 mm in width and 40 mm in length, and a cylindrical container, having an inner diameter of 40 mm, as shown in Fig. 3. The inner wall of the container was profiled with grooves in such a way that the asperity was larger than the largest particle in the mortar sample being tested. This was to minimise slippage of the mortar at the container surface during shearing.

At the onset of the test, the shear vane was concentrically inserted into the mortar sample in the cylindrical container and then set to rotate at controlled rotation speed, following a shearing sequence which consisted of two shearing cycles. The first cycle, called the pre-shearing cycle, was to apply pre-shearing so that all the samples tested had the same shearing history before measurement. The second cycle, called the data-logging cycle, was for the actual measurement. In each cycle, the rotation speed was increased from 0 to 50 rpm in 75 s and then decreased to 0 rpm in another 75 s. During the data-logging cycle, the torque induced at the shear vane was continuously monitored and regularly logged. The results obtained at decreasing rotation speed, which are generally more consistent and repeatable, were used for evaluating the rheological properties of the mortar sample.

As the mortar is non-Newtonian, it is customary to describe its rheological properties by either the Bingham model (which assumes that the shear stress–shear rate curve is linear) or the Herschel–Bulkley model (which assumes that the shear stress–shear rate curve follows the power equation). Upon curve fitting using both models, it was found that the experimental results agreed better with the Herschel–Bulkley model, whose shear stress–shear rate relation is given by:

$$\tau = \tau_0 + k(\dot{\gamma})^n \quad (1)$$

where $\tau$ is the shear stress (Pa), $\tau_0$ is the yield stress (Pa), $\dot{\gamma}$ is the shear rate ($s^{-1}$), and $k$ ($Pas^n$) and $n$ (non-dimensional) are the empirical coefficients. To evaluate the rheological properties of the mortar sample tested, the best-fit curve based on the above equation was first obtained by regression analysis. Then, from the best-fit curve so obtained, the yield stress (taken as the shear stress at a shear rate of zero) and apparent viscosity (taken as the ratio of shear stress to shear rate at a shear rate of 14 $s^{-1}$) were determined to characterize the rheology of the mortar sample.

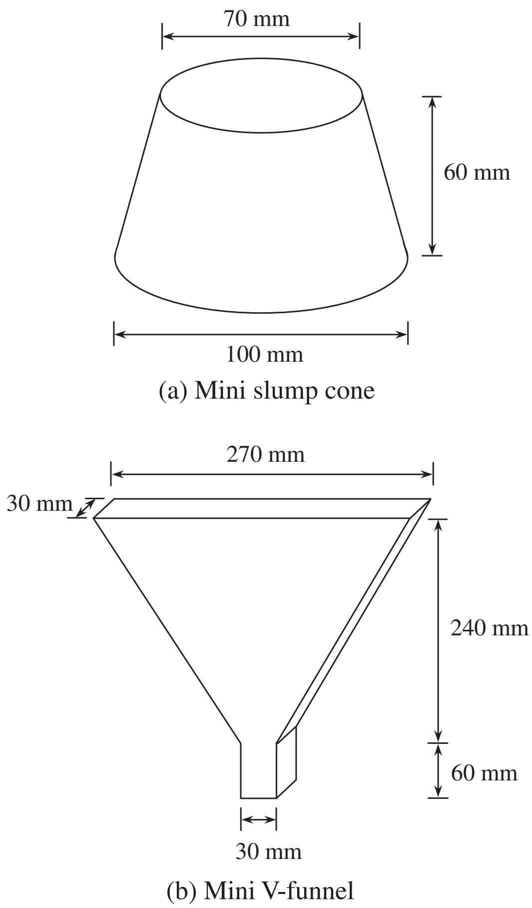


**Fig. 2.** Mini slump cone and mini V-funnel.

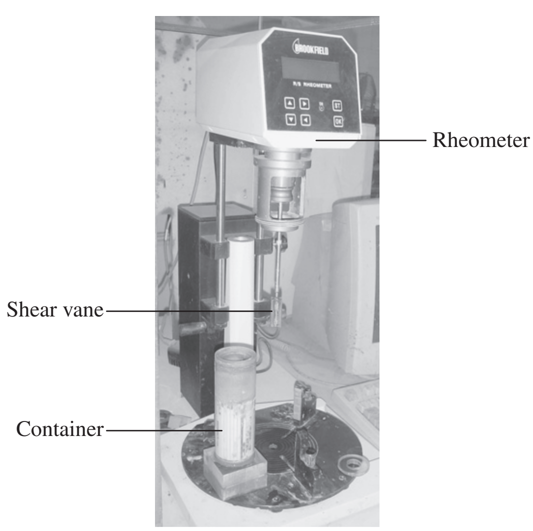


**Fig. 3.** Rheometer, shear vane and container.

*4.3. Measuring cohesiveness*

The cohesiveness of each mortar sample was measured using a micro version of the sieve segregation test for self-consolidating concrete (SCC) stipulated in the European Guidelines for SCC [22]. This sieve segregation test for mortar is similar to the sieve segregation test for SCC except that a smaller 1.18 mm sieve is employed.

For carrying out the test, an approximately 0.2 l mortar sample was poured onto the 1.18 mm sieve from a height of 300 mm. After 2 min, the mortar dripped through the sieve and collected by a base receiver was weighed. For a mortar with low cohesiveness, nearly all the mortar poured onto the sieve dripped through the sieve. On the contrary, for a mortar with high cohesiveness, only a small amount of mortar dripped through the sieve. Hence, the proportion of mortar dripped through the sieve may be taken as a measure of cohesiveness (a larger proportion indicates a low cohesiveness and vice versa). Following the sieve segregation test for SCC, the sieve segregation index (SSI) of the mortar tested may be determined as:

$$\mathrm{SSI} = \frac{M_p}{M_m} \times 100\% \tag{2}$$

in which $M_p$ is the mass of mortar dripped through the sieve and collected by the base receiver and $M_m$ is the mass of mortar poured onto the sieve.

*4.4. Measuring packing density*

The wet packing test developed by the author's research group [6–8] was used to measure the packing density of the solid particles in the mortar. Basically, the wet packing test measures the solid concentrations of the solid particles at different W/S ratios and determines the packing density of the solid particles as the maximum solid concentration so obtained. Compared to the conventional dry packing tests, this wet packing test has the advantage that the effects of water and SP are incorporated because the measurement is conducted with water and SP added. In this particular case, since the cement to fine aggregate ratio was fixed and the solid compositions of the 35 mortar samples were the same, the only factor that might affect the packing density of the solid particles was the variation in SP dosage. To study the effect of SP dosage, the wet packing test was conducted for each SP dosage adopted.

## 5. Results and discussions

*5.1. Flow spread and flow rate*

The flow spread and flow rate results are tabulated in the second and third columns of Table 1 and plotted against the W/S ratio for different SP dosages in Fig. 4. From the figure, it can be seen that at a given SP dosage, both the flow spread and flow rate started to increase from zero as the W/S ratio was increased to beyond a certain value. Then, the flow spread and flow rate increased continuously with the W/S ratio but in different manners. The flow spread increased with the W/S ratio at a decreasing rate until eventually at flow spread larger than 250 mm, the flow spread increased only marginally with the W/S ratio. On the contrary, the flow rate increased steadily with the W/S ratio in a more or less linear manner.

Comparing the different curves at different SP dosages, it is evident that the W/S ratio at which the flow spread and flow rate started to increase from zero was dependent on the SP dosage. When no SP was added, the mortar did not flow until the W/S ratio was increased to as high as 0.70. When SP was added at a dosage of 0.5%, the mortar started to flow when the W/S ratio was increased to 0.50. When SP was added at a higher dosage of 1.0%, the mortar started to flow when the W/S ratio was increased to 0.40. Hence, the addition of SP would render the mortar flowable at a lower W/S ratio. Moreover, the upward shifting of the flow spread and flow rate curves as the SP dosage was increased indicates that both the flow spread and flow rate generally increased with the SP dosage. However, the flow spread increased significantly only until the

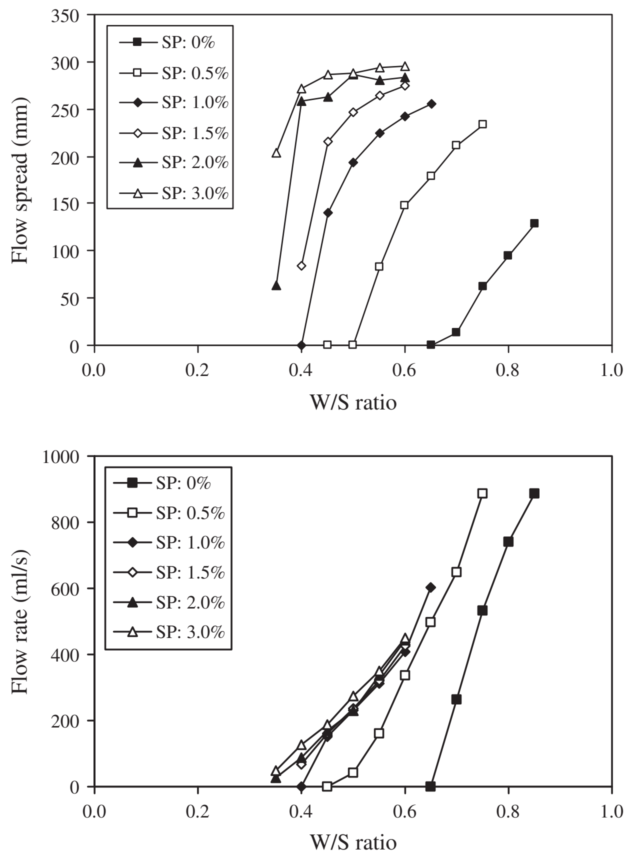


**Fig. 4.** Flowability versus W/S ratio.

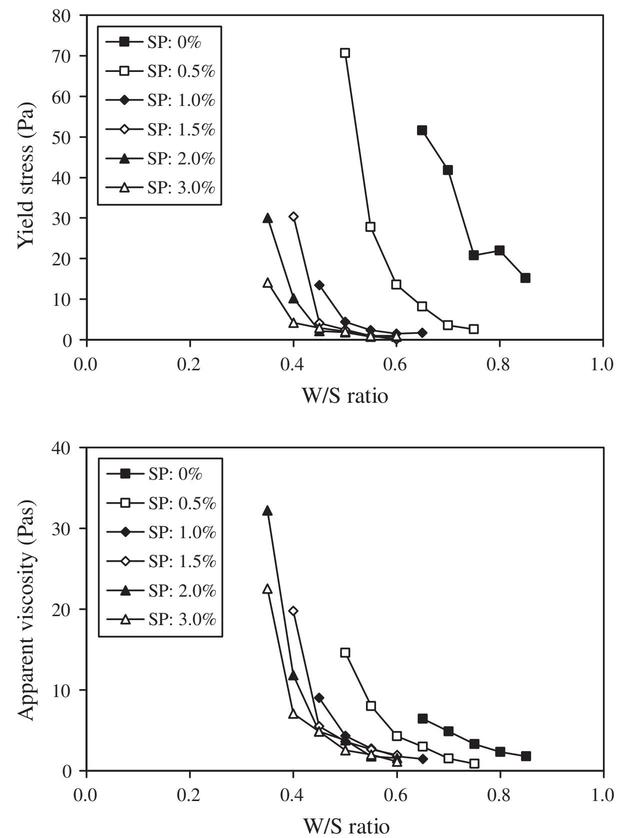


**Fig. 5.** Rheological properties versus W/S ratio.

SP dosage was increased to 2.0% and the flow rate increased significantly only until the SP dosage was increased to 1.0%.

### 5.2. Yield stress and apparent viscosity

The yield stress and apparent viscosity results are tabulated in the fourth and fifth columns of Table 1 and plotted against the W/S ratio for different SP dosages in Fig. 5. From the figure, it can be seen that both these two rheological properties gradually decreased as the W/S ratio was increased.

Comparing the different curves at different SP dosages, it is evident that the yield stress and apparent viscosity also varied with the SP dosage. When the SP was first added at a dosage of 0.5%, both the yield stress and apparent viscosity were substantially reduced. For instance, at a W/S ratio of 0.65, the yield stress was reduced by about 80% whereas the apparent viscosity was reduced by about 50%. When the SP dosage was increased to 1.0%, significant further reductions in the yield stress and apparent viscosity were achieved. However, after the SP dosage was increased to beyond 1.0%, the further reductions in the yield stress and apparent viscosity gradually diminished. Specifically, at W/S ratios higher than 0.5, the further reductions in the yield stress and apparent viscosity became minimal when the SP dosage was increased to higher than 2.0% and 1.0%, respectively.

### 5.3. Cohesiveness

The sieve segregation index (SSI) results are tabulated in the sixth column of Table 1 and plotted against the W/S ratio for different SP dosages in Fig. 6. From the figure, it can be seen that at a given SP dosage, the SSI started to increase from zero as the W/S ratio was increased to beyond a certain value depending on the SP dosage. Then, the SSI increased steadily with the W/S ratio. This implies that an increase in water content would impair the cohesiveness of mortar. Comparing the different curves at different SP dosages, it is evident that the variation of the SSI with the W/S ratio is highly dependent on the SP dosage. Generally, the SSI–W/S ratio curve is higher at a higher SP dosage, indicating that the SSI increased not only with the W/S ratio, but also with the SP dosage.

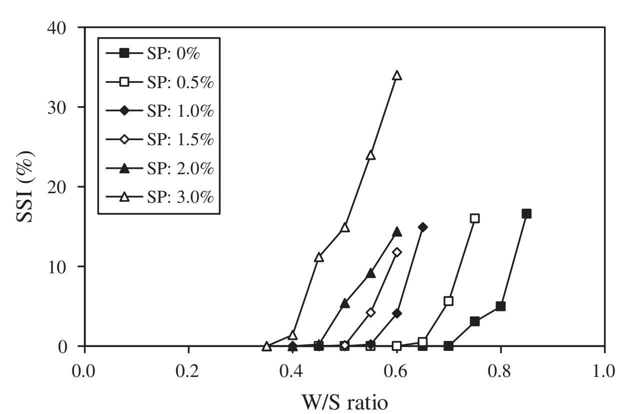


**Fig. 6.** Sieve segregation index versus W/S ratio.

### 5.4. Correlations between flowability and rheological properties

To study the relationship between the flowability and rheological properties, the flow spread and flow rate are respectively

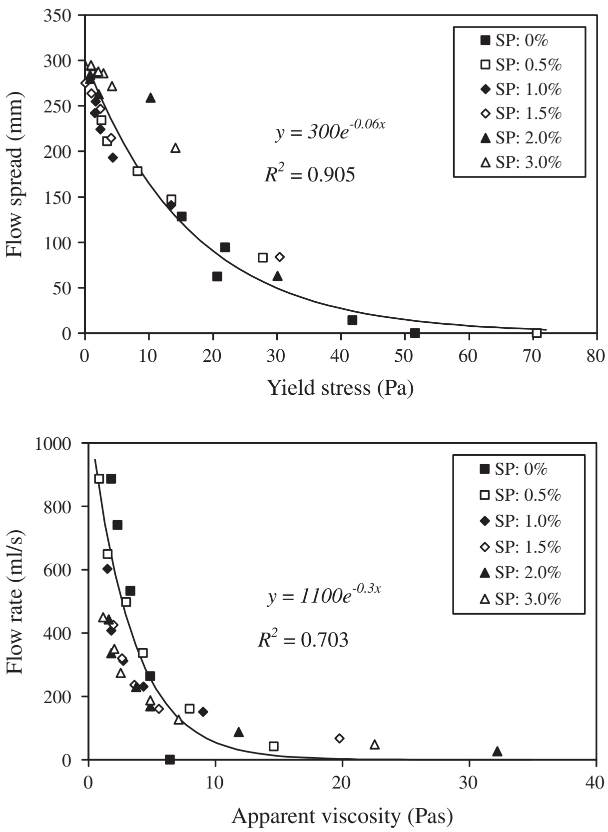


**Fig. 7.** Correlations between flowability and rheological properties.

**Table 2**
Packing density and water film thickness of the mortar samples.

| Sample number | Packing density | Excess water ratio | Specific surface area ($m^2/m^3$) | Water film thickness (μm) |
|---|---|---|---|---|
| 0–0.65 | 0.662 | 0.139 | 780,200 | 0.178 |
| 0–0.70 | | 0.189 | | 0.242 |
| 0–0.75 | | 0.239 | | 0.306 |
| 0–0.80 | | 0.289 | | 0.370 |
| 0–0.85 | | 0.339 | | 0.434 |
| 0.5–0.45 | 0.689 | −0.001 | | −0.002 |
| 0.5–0.50 | | 0.049 | | 0.062 |
| 0.5–0.55 | | 0.099 | | 0.126 |
| 0.5–0.60 | | 0.149 | | 0.191 |
| 0.5–0.65 | | 0.199 | | 0.255 |
| 0.5–0.70 | | 0.249 | | 0.319 |
| 0.5–0.75 | | 0.299 | | 0.383 |
| 1.0–0.40 | 0.707 | −0.014 | | −0.018 |
| 1.0–0.45 | | 0.036 | | 0.046 |
| 1.0–0.50 | | 0.086 | | 0.110 |
| 1.0–0.55 | | 0.136 | | 0.174 |
| 1.0–0.60 | | 0.186 | | 0.238 |
| 1.0–0.65 | | 0.236 | | 0.302 |
| 1.5–0.40 | 0.719 | 0.009 | | 0.012 |
| 1.5–0.45 | | 0.059 | | 0.076 |
| 1.5–0.50 | | 0.109 | | 0.140 |
| 1.5–0.55 | | 0.159 | | 0.204 |
| 1.5–0.60 | | 0.209 | | 0.268 |
| 2.0–0.35 | 0.725 | −0.029 | | −0.038 |
| 2.0–0.40 | | 0.021 | | 0.027 |
| 2.0–0.45 | | 0.071 | | 0.091 |
| 2.0–0.50 | | 0.121 | | 0.155 |
| 2.0–0.55 | | 0.171 | | 0.219 |
| 2.0–0.60 | | 0.221 | | 0.283 |
| 3.0–0.35 | 0.729 | −0.022 | | −0.028 |
| 3.0–0.40 | | 0.028 | | 0.036 |
| 3.0–0.45 | | 0.078 | | 0.100 |
| 3.0–0.50 | | 0.128 | | 0.164 |
| 3.0–0.55 | | 0.178 | | 0.228 |
| 3.0–0.60 | | 0.228 | | 0.293 |

*Note*: In the sample number X–Y, X denotes the SP dosage as a percentage by mass of the cementitious materials and Y denotes the W/S ratio by volume.

plotted against the yield stress and apparent viscosity in Fig. 7. From these plots, it can be seen that there exist a good correlation between the flow spread and yield stress with a $R^2$ value of 0.905 and also a good correlation between the flow rate and apparent viscosity with a $R^2$ value of 0.703. Hence, the flow spread is governed mainly by the yield stress while the flow rate is governed mainly by the apparent viscosity. The good correlations obtained suggest that the flow spread and flow rate, which can be measured more easily, may be taken as alternative measures of the yield stress and apparent viscosity.

## 6. Roles of water film thickness and SP dosage

### 6.1. Packing density

The packing density results of the solid particles in the mortar at different SP dosages are tabulated in the second column of Table 2 and plotted against the SP dosage in Fig. 8. From the figure, it can be seen that the packing density increased significantly with the SP dosage. With no SP added, the packing density was only 0.662. When the SP was first added at a dosage of 0.5%, the packing density increased to 0.689. When the SP dosage was increased to 1.0% and 2.0%, the packing density increased to 0.707 and 0.725, respectively. However, after the SP dosage was increased to beyond 2.0%, there was little further increase in packing density.

The above results reveal that there exists a saturation SP dosage beyond which the packing density would increase only marginally with the SP dosage. In the present case, the saturation SP dosage may be determined as 2.0%. Furthermore, there exists a maximum packing density achievable only at a SP dosage equal to or higher than the saturation SP dosage. In the present case, the maximum packing density may be taken as 0.729, which is about 10% higher than that with no SP added.

### 6.2. Excess water ratio and water film thickness

From the packing density, which is hereafter denoted by $\phi$, the voids ratio $u$ (defined as voids volume to solid volume ratio) may be calculated as $u = (1-\phi)/\phi$ and the excess water ratio $u'_w$ (defined as excess water volume to solid volume ratio) may be calculated as $u'_w = u_w - u$, in which $u_w$ is the water ratio (same as the W/S ratio by volume). The excess water ratios so obtained are tabulated in the third column of Table 2. It is noteworthy that although the packing density increased by only several percent when SP was added, such increase in packing density can have significant effect on the excess water ratio. For instance, despite added with the same water content, mix 0.5–0.45, which has a packing density of 0.689, is calculated to have an excess water ratio of −0.001 (a negative excess water ratio means that the water added was not sufficient to fill up the voids in the mortar leading to the presence of air in the voids), while mix 1.0–0.45, which has a packing density of 0.707, is calculated to have an excess water ratio of 0.036.

Further, from the specific surface areas of the cement and fine aggregate, the solid surface area of the mortar can be calculated, and from the excess water ratio, the WFT may be determined as the excess water to solid surface area ratio. The solid surface area and WFT so obtained for each mortar sample are tabulated in the fourth and fifth columns of Table 2. For the mortar samples tested, the WFT ranged from −0.038 to 0.434 μm. When positive, the WFT has the physical meaning of the average thickness of the water films coating the particles. However, when negative, the WFT no longer has such physical meaning. A negative WFT means that the water added was not sufficient to fill up the voids in the mortar

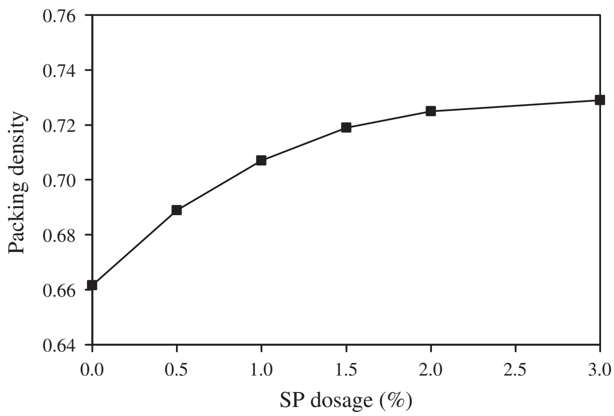


**Fig. 8.** Packing density results.

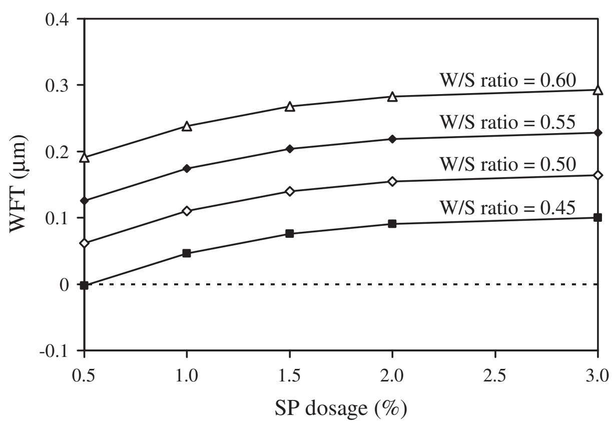


**Fig. 9.** WFT versus SP dosage.

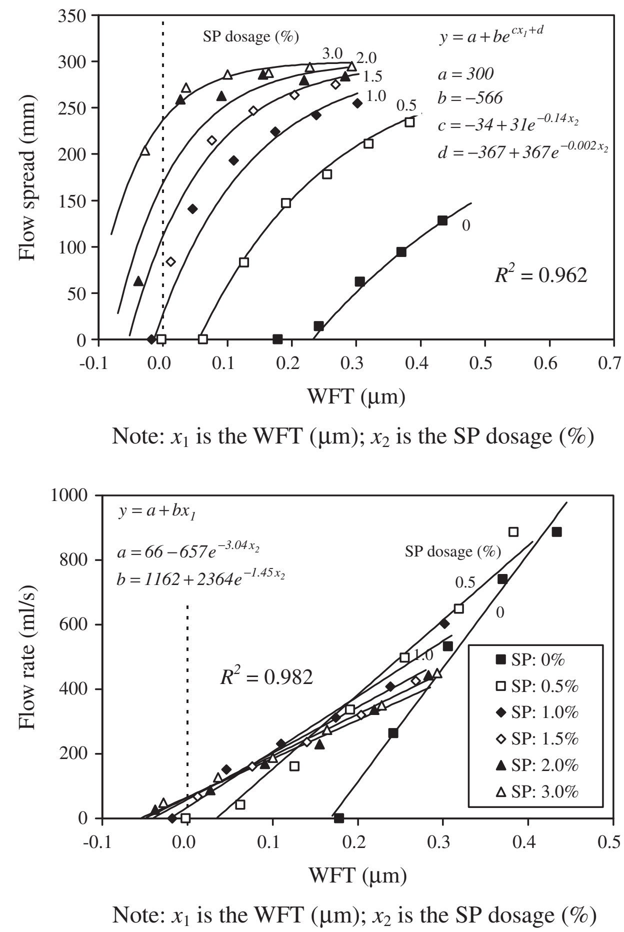


**Fig. 10.** Flowability versus WFT.

leading to the presence of air in the voids. To illustrate how the WFT varied with the W/S ratio and SP dosage, the WFT is plotted against the SP dosage for W/S ratios of 0.45, 0.50, 0.55 and 0.60 in Fig. 9. The curves plotted reveal that the WFT increased significantly with the SP dosage at a decreasing rate and was always higher at a higher W/S ratio.

### *6.3. Combined effects of WFT and SP dosage on flow spread*

The flow spread is plotted against the WFT for different SP dosages in the upper half of Fig. 10. It is seen first of all that the variation of flow spread with the WFT was highly dependent on the SP dosage. At a lower SP dosage, the flow spread started to increase from zero at a relatively large WFT and thereafter increased at a relatively slow rate with the WFT. At a higher SP dosage, the flow spread started to increase from zero at a relatively small WFT and thereafter increased at a relatively fast rate with the WFT. More generally, at the same WFT, the flow spread increased quite substantially with the SP dosage. This suggests that although the effect of SP on packing density has been reflected in the WFT, the SP by itself has certain direct effect on the flow spread. To study the combined effects of WFT and SP dosage, multi-variable regression analysis was carried out to derive the best-fit curves at different SP dosages, as plotted alongside the data points. The regression analysis yielded a very high $R^2$ value of 0.962, indicating that the flow spread was governed mainly by the WFT and SP dosage.

The direct effect of SP not reflected by the WFT was probably caused by the dispersive action of the SP. With no or little SP added, the solid particles attracted each other and as a result the mortar appeared to be cohesive and reluctant to flow. However, with more SP added, the solid particles were dispersed, thus rendering the mortar less cohesive and more ready to flow. During the mini slump cone tests, it was observed that at a higher SP dosage, the mortar patty formed was generally thinner. Since the volume of mortar sample was constant, the smaller thickness of the mortar patty might have caused the observed larger flow spread at higher SP dosage. Lastly, it is also seen that when the SP dosage was increased to 2.0% or higher, the SP dosage had little effect and the WFT became the sole factor governing the flow spread.

### *6.4. Combined effects of WFT and SP dosage on flow rate*

The flow rate is plotted against the WFT for different SP dosages in the lower half of Fig. 10. It is seen that at a given SP dosage, the flow rate increased steadily with the WFT in a more or less linear manner. However, the WFT at which the flow rate started to increase and the rate of increase of flow rate with the WFT were highly dependent on the SP dosage. At a lower SP dosage, the flow rate started to increase from zero at a relatively large WFT and thereafter increased at a relatively fast rate with the WFT. At a higher SP dosage, the flow rate started to increase from zero at a relatively small WFT and thereafter increased at a relatively slow rate with the WFT. Hence, the SP by itself has certain direct effect on the flow rate but its effect on flow rate is quite different from that on flow spread. To study the combined effects of WFT and SP dosage, multi-variable regression analysis was carried out to derive the best-fit curves at different SP dosages, as plotted alongside the data points. The regression analysis yielded a very high $R^2$

value of 0.982, indicating that the flow rate was governed mainly by the WFT and SP dosage.

As for the case of flow spread, the direct effect of SP on flow rate not reflected by the WFT was probably due to the dispersive action of the SP. With no or little SP added, the mortar appeared to be cohesive and reluctant to flow, thus leading to a relatively low flow rate. However, with more SP added, the mortar became less cohesive and more ready to flow, thus leading to a relatively high flow rate. Lastly, it is also seen that when the SP dosage was increased to 1.0% or higher, the SP dosage had little effect and the WFT became the sole factor governing the flow rate.

### 6.5. Combined effects of WFT and SP dosage on yield stress

The yield stress is plotted against the WFT for different SP dosages in the upper half of Fig. 11. It is seen that the yield stress decreased as the WFT increased. However, the variation of yield stress with the WFT was highly dependent on the SP dosage. Generally, at a lower SP dosage, the effect of SP dosage was larger while at a higher SP dosage, the effect of SP dosage was smaller. Nevertheless, it is obvious that the SP by itself has certain direct effect on the yield stress. To study the combined effects of WFT and SP dosage, multi-variable regression analysis was carried out to derive the best-fit curves at different SP dosages, as plotted alongside the data points. The regression analysis yielded a very high $R^2$ value of 0.884, indicating that the yield stress was governed mainly by the WFT and SP dosage. Lastly, it is also seen that when the SP dosage was increased to 2.0% or higher, the SP dosage had little effect and the WFT became the sole factor governing the yield stress.

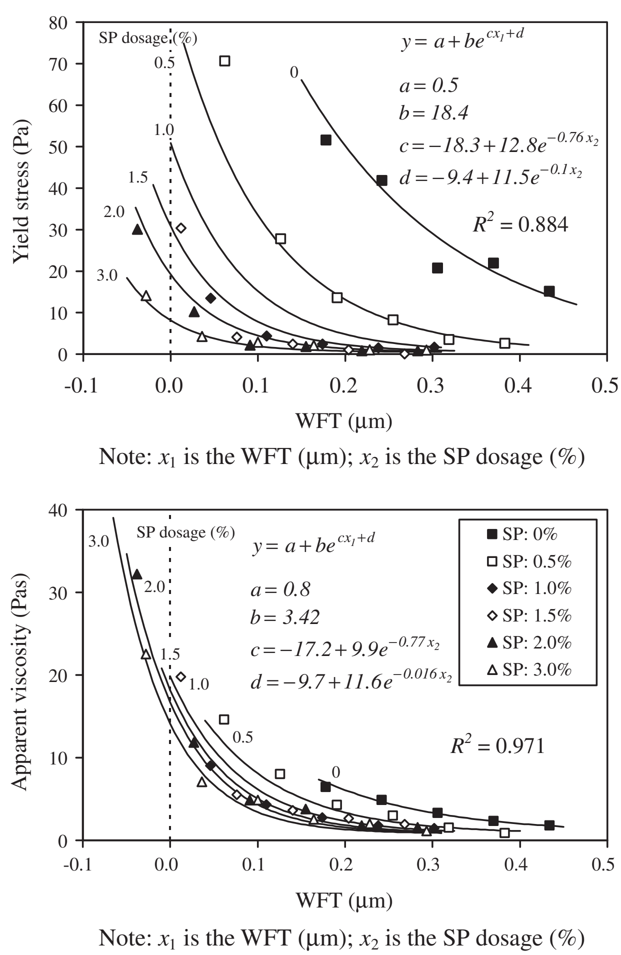


**Fig. 11.** Rheological properties versus WFT.

### 6.6. Combined effects of WFT and SP dosage on apparent viscosity

The apparent viscosity is plotted against the WFT for different SP dosages in the lower half of Fig. 11. It is seen that as for the yield stress, the apparent viscosity decreased as the WFT increased. Furthermore, the variation of apparent viscosity with the WFT was also dependent on the SP dosage. As before, the effect of SP dosage was larger when the SP dosage was relatively low and smaller when the SP dosage was relatively high. To study the combined effects of WFT and SP dosage, multi-variable regression analysis was carried out to derive the best-fit curves at different SP dosages, as plotted alongside the data points. The regression analysis yielded a very high $R^2$ value of 0.971, indicating that the apparent viscosity was governed mainly by the WFT and SP dosage. Lastly, it is also seen that when the SP dosage was increased to 1.0% or higher, the SP dosage had little effect and the WFT became the sole factor governing the apparent viscosity.

### 6.7. Combined effects of WFT and SP dosage on cohesiveness

The SSI is plotted against the WFT for different SP dosages in Fig. 12 to illustrate the combined effects of WFT and SP dosage on cohesiveness. In general, the SSI increased steadily with both the WFT and SP dosage. Furthermore, from the large separation between the SSI–WFT curves for different SP dosages, it can be seen that the effect of SP dosage on SSI remained large even at comparatively high SP dosage. Hence, unlike the effects of SP dosage on rheology, which became very small when the SP dosage was increased to beyond a certain saturation SP dosage, the effect of SP dosage on SSI or cohesiveness showed no saturation.

From the above results, it may be inferred that there is no definite saturation SP dosage causing segregation. Since the SSI increases with both the WFT and SP dosage, both the WFT and SP dosage should be limited to avoid segregation. The limit to be imposed on the SP dosage should be lower when the WFT is relatively large and higher when the WFT is relatively small. On the other hand, the limit to be imposed on the WFT should be smaller when the SP dosage is relatively high and larger when the SP dosage is relatively low. More research along this line to produce practical guidelines for the avoidance of segregation is recommended.

## 7. Effect of SP under different shear rates

From the above observations and detailed analysis, it is evident that the addition of a SP has two major effects: (1) the agglomeration reduction effect, which increases the packing density of the solid particles and consequently increases the WFT; and (2) the cohesiveness reduction effect, which renders the mortar less cohesive and

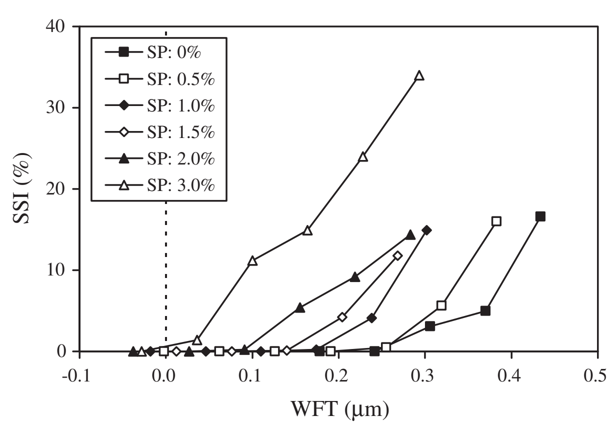


**Fig. 12.** Sieve segregation index versus WFT.

thus more ready to flow. The first effect is evidenced by the increase of WFT with the SP dosage while the second effect is reflected by the increase of flowability with the SP dosage at the same WFT.

However, the flow spread, flow rate, yield stress and apparent viscosity seem to be affected by the cohesiveness reduction effect to different extents. Comparatively, the flow spread and yield stress are more sensitive to the cohesiveness change of the mortar, as depicted by the widely separated flow spread–WFT curves in Fig. 10 and the widely separated yield stress–WFT curves in Fig. 11. In contrast, the flow rate and apparent viscosity are less sensitive to the cohesiveness change of the mortar, as depicted by the closely spaced flow rate–WFT curves in Fig. 10 and the closely spaced apparent viscosity–WFT curves in Fig. 11. Nevertheless, for each of these flowability and rheological parameters, there appears to be a saturation SP dosage beyond which the SP dosage has little effect. Within the range of mix composition tested in this particular study, the saturation SP dosage for maximum flow spread and minimum yield stress is about 2% and the saturation SP dosage for maximum flow rate and minimum apparent viscosity is about 1%.

The above phenomena may be attributed to the different shear rates involved during the tests. Basically, the shear rate during the mini slump cone test is in the range of 0.01–1 $s^{-1}$ and the shear rate during the mini V-funnel test is in the range of 1 to 40 $s^{-1}$ [23]. On the other hand, the shear rates for the determination of the yield stress (which characterizes the rheology in static state) and the apparent viscosity (which characterizes the rheology in dynamic state) are zero and 14 $s^{-1}$, respectively. Overall, it may be said that the flow spread and yield stress are more representative of the rheology of mortar at low shear rate, and the flow rate and apparent viscosity are more representative of the rheology of mortar at high shear rate. As the flow spread and yield stress are more sensitive to cohesiveness change and the flow rate and apparent viscosity are less sensitive to cohesiveness change, it may be inferred that the cohesiveness reduction due to the addition of SP has greater effects on the flowability and rheology of mortar at a lower shear rate and smaller effects at a higher shear rate.

The different effects of SP under different shear rates may be explained below. By dispersing the solid particles in the mortar, the SP added would significantly reduce the cohesiveness of the mortar and the resistance caused by cohesiveness, thereby leading to a higher flow spread and a lower yield stress. However, as the shear rate increases, the solid particles in the mortar would collide with each other, thus causing substantial resistance to be developed. At a higher shear rate, the frequency of particle collision should be higher and consequently the resistance caused by particle collision should also be higher. Hence, at a relatively high shear rate, both the resistance caused by cohesiveness and the resistance caused by particle collision would resist the flow. Since the resistance caused by cohesiveness is then only part of the resistance to flow, the cohesiveness reduction due to the addition of SP has smaller effects at a higher shear rate.

## 8. Conclusions

A total of 35 cement–sand mortar samples proportioned with different W/S ratios and different SP dosages were produced for flowability, rheology, cohesiveness and packing density measurements. The flowability was measured in terms of flow spread and flow rate using the mini slump cone and mini V-funnel tests, the rheology was measured in terms of yield stress and apparent viscosity using a speed-controlled rheometer, the cohesiveness was measured using a micro version of the sieve segregation test, and the packing density was measured under wet condition using the newly developed wet packing method with the effects of water and SP incorporated. Overall, the test results revealed that both the W/S ratio and SP dosage have major effects on the flowability, rheology and cohesiveness of mortar whereas the SP dosage has significant effect on the packing density of mortar.

As expected, the flowability and rheology were improved but the cohesiveness was impaired when the W/S ratio and/or the SP dosage were increased. The effects of SP dosage on the flowability and rheology showed obvious saturation when the SP dosage was increased to beyond a certain saturation dosage but the effect of SP dosage on cohesiveness showed no saturation. Moreover, correlation of the flow spread and flow rate respectively to the yield stress and apparent viscosity indicated that the flow spread and flow rate are more or less equivalent to the yield stress and apparent viscosity and may therefore be taken as alternative measures of the yield stress and apparent viscosity. From the measured packing density and solid surface area, the WFT of each mortar sample was evaluated. It was found that because of gradual improvement in packing density due to the agglomeration reduction effect of SP, the WFT increased significantly with the SP dosage. By plotting the flow spread, flow rate, yield stress and apparent viscosity against the WFT and SP dosage, it was also found that at a low SP dosage, these flowability and rheological parameters are dependent on both the WFT and SP dosage while at a high SP dosage, they are dependent solely on the WFT.

To study the combined effects of the WFT and SP dosage, multivariable regression analysis was carried out. Correlations of the flow spread, flow rate, yield stress and apparent viscosity to both the WFT and SP dosage yielded $R^2$ values of 0.962, 0.982, 0.884 and 0.971, respectively. Such high $R^2$ values suggest that the WFT and SP dosage are the major factors governing the flowability and rheology of mortar. Finally, based on the observed phenomena, it may be concluded that the addition of a SP has two major effects: the agglomeration reduction effect which increases the packing density and WFT; and the cohesiveness reduction effect which increases the flowability of mortar at the same WFT. Furthermore, the cohesiveness reduction due to the addition of SP has greater effects on the flowability and rheology of mortar at a lower shear rate and smaller effects at a higher shear rate. Such influence of the shear rate is probably due to the increase in particle collision with the shear rate, which causes substantial resistance to flow and renders the resistance caused by the cohesiveness relatively less important. In any case, the WFT remains the key factor to be considered in the mix design of the mortar portion of concrete.

## Acknowledgment

The work described in this paper was fully supported by a Grant from the Research Grants Council of the Hong Kong Special Administrative Region, China (Project No. 713309).

## References

[1] Mehta PK, editor. In: Proceedings of Mario Collepardi symposium on advances in concrete science and technology. 5th CANMET/ACI international conference on superplasticizers and other chemical admixtures, Rome; 1997.
[2] Mindess S, Young JF, Darwin D. Concrete. 2nd ed. New Jersey, USA: Prentice Hall; 2003 [chapter 8. p. 176–82].
[3] Ramachandran VS, editor. Concrete Admixtures Handbook: Properties, Science, and Technology. 2nd ed. Berlin: Science; 1996.
[4] Neville AM. Properties of concrete. 4th ed. England: Longman; 1995 [chapter 13].
[5] Svarovsky L. Powder testing guide: methods of measuring the physical properties of bulk powders. England: Elsevier Applied Science Publishers Ltd; 1987.
[6] Wong HHC, Kwan AKH. Packing density of cementitious materials: Part 1 – Measurement using a wet packing method. Mater Struct 2008;41(4):689–701.
[7] Fung WWS, Kwan AKH, Wong HHC. Wet packing of crushed rock fine aggregate. Mater Struct 2009;42(5):631–43.
[8] Kwan AKH, Fung WWS. Packing density measurement and modelling of fine aggregate and mortar. Cem Concr Compos 2009;31(6):349–57.

[9] Zingg A, Winnefeld F, Holzer L, Pakusch J, Becker S, Figi R, et al. Interaction of polycarboxylate-based superplasticizers with cements containing different $C_3A$ amounts. Cem Concr Compos 2009;31(3):153–62.
[10] Helmuth RA. Structure and rheology of fresh cement paste. In: Proceedings of 7th international congress of chemistry of cement: sub-theme VI-0; 1980. p. 16–30.
[11] Zhang C, Wang A, Tang M, Liu X. The filling role of pozzolanic material. Cem Concr Res 1996;26(6):943–7.
[12] Nanthagopalan P, Haist M, Santhanam M, Müller HS. Investigation on the influence of granular packing on the flow properties of cementitious suspensions. Cem Concr Compos 2008;30(9):763–8.
[13] Peng Y, Hu S, Ding Q. Dense packing properties of mineral admixtures in cementitious material. Particuology 2009;7(5):399–402.
[14] Kwan AKH, Wong HHC. Effects of packing density, excess water and solid surface area on flowability of cement paste. Adv Cem Res 2008;20(1):1–11.
[15] Wong HHC, Kwan AKH. Rheology of cement paste: role of excess water to solid surface area ratio. J Mater Civ Eng 2008;20(2):189–97.
[16] Kwan AKH, Fung WWS, Wong HHC. Water film thickness, flowability and rheology of cement–sand mortar. Adv Cem Res 2010;22(1):3–14.
[17] Fung WWS, Kwan AKH. Role of water film thickness in rheology of CSF mortar. Cem Concr Compos 2010;32(4):255–64.
[18] Gołaszewski J, Szwabowski J. Influence of superplasticizers on rheological behaviour of fresh cement mortars. Cem Concr Res 2004;34(2):235–48.
[19] Aïtcin PC. High-performance concrete. London: E&FN Spon; 1998. Chapters 8, 9.
[20] Wong HHC, Kwan AKH. Packing density of cementitious materials: measurement and modelling. Mag Concr Res 2008;60(3):165–75.
[21] Okamura H, Ouchi M. Self-compacting concrete. J Adv Concr Technol 2003;1(1):5–15.
[22] SCC European Project Group. The European guidelines for self-compacting concrete. BIBM, CEMBUREAU, EFCA, EFNARC and ERMCO; 2005. p. 63.
[23] Artelt C, Garcia E. Impact of superplasticizer concentration and of ultra-fine particles on the rheological behaviour of dense mortar suspensions. Cem Concr Res 2008;38(5):633–42.